MINERALOGICAL MAGAZINE, JUNE 1986, VOL. 50, PP. 257-66

Muscovite solid solutions in the system K_2O-MgO-FeO-Al_2O_3-SiO_2-H_2O: an experimental study at 2 kbar P_{H_2O} and comparison with natural Li-free white micas

GILLES MONIER

Laboratoire de Pétrologie, Université d'Orléans, 45046 Orléans Cedex, France

AND

JEAN-LOUIS ROBERT

Centre de Recherche sur la Synthèse et Chimie des Minéraux, G.I.S. C.N.R.S.-B.R.G.M., 1A rue de la Férollerie, 45071 Orléans Cedex 2, France

ABSTRACT. This paper presents the results of an experimental study of muscovite solid solutions in the system K_2O-$M^{2+}O$-Al_2O_3-SiO_2-H_2O-(HF), with M^{2+} = Mg^{2+} or Fe^{2+}, in the temperature range 300–700 °C under 2 kbar P_{H_2O}. Muscovite solid solutions can be described, in this system, as the result of two substitutions. One is the phengitic substitution (x), which preserves the pure dioctahedral character of the mica; the second is the biotitic substitution (y), which leads to trioctahedral micas and does not change the composition of the tetrahedral layer Si_3Al. The general formula of muscovite in this system is $K(Al_{2-x-2y/3}M^{2+}_{x+y}\square_{1-y/3})(Si_{3+x}Al_{1-x})O_{10}(OH,F)_2$. Both substitutions x and y are more extensive at lower temperatures. The extent of solid solution decreases drastically with increasing temperature.

For $T > 600$ °C, the phengitic substitution (x) becomes negligible, but some biotitic substitution (y) persists. This unsymmetrical decrease of the solid solution of muscovite with increasing temperature is similar to that previously observed in phlogopite, the micas with a tetrahedral layer composition of Si_3Al being the most stable. The behaviour of muscovite solid solutions in the ferrous system is qualitatively identical to that observed in the magnesian one, but the extent of solid solution is smaller than with Mg^{2+}. Fluorine neither changes the size nor the shape of the solid solution fields but increases their stability by about 50 °C.

A comparison of these experimental results with data on natural muscovites is presented. Most natural primary (magmatic) granitic muscovites lie very close to the muscovite end member, in agreement with their high-temperature origin. Low-temperature muscovites (300–400 °C), typically muscovites from hydrothermally altered granitic rocks, can have high x and y values. The rate of the biotitic substitution y can reach 0.6, which corresponds to an octahedral occupancy of 2.2 atoms per formula unit (based on 11 oxygens), consistent with the experimental data.

KEYWORDS: muscovite, phengite, solid solution, crystal-chemistry, experimental mineralogy, granites, hydrothermal alteration.

NATURAL lithium-free white micas are generally described as solid solutions between the muscovite end member $K(Al_2\square)(Si_3Al)O_{10}(OH)_2$, where $\square$ stands for an octahedral vacant site, and the celadonite end member $K(AlM^{2+}\square)Si_4O_{10}(OH)_2$, with M^{2+} = Mg^{2+}, Fe^{2+}, thus, they are considered to belong to the so-called phengitic series. The substitutional mechanism which describes this series can be written

$$Al^{VI},Al^{IV} \rightleftharpoons (M^{2+})^{VI},Si^{IV}. \quad (1)$$

If x is the amount of substitution, according to equation (1), the muscovite end member has $x = 0$ and the Al-celadonite end member has $x = 1$. The purely dioctahedral character is maintained. This series has been the subject of several experimental investigations (Crowley and Roy, 1964; Velde, 1965, 1980; Green, 1981) and of many studies of micas in metamorphic rocks. These works show an increase of the extent of the phengitic substitution [mechanism (1)] with increasing water pressure. The possibility of solid solution between dioctahedral and trioctahedral micas has been rarely considered; this kind of solid solution involves a second substitutional mechanism:

$$2/3Al^{VI},1/3\square^{VI} \rightleftharpoons (M^{2+})^{VI}. \quad (2)$$

If y is the amount of substitution, according to equation (2), the muscovite end member has $y = 0$ and the biotite end member (phlogopite with

M^{2+} = Mg and annite with M^{2+} = Fe^{2+}), has $y = 3$, with the formula $KM_3^{2+}(Si_3Al)O_{10}(OH)_2$.

In this series, the number of octahedral vacant sites is variable. Recently, Massonne (1981) has taken this possibility into account in his experimental work on phengites between 5 and 30 kbar. It is noteworthy that most natural muscovite solid solutions are combinations of substitutions (1) and (2) and can be described by the two parameters (x, y). So, the general formula of muscovites is $K(Al_{2-x-2y/3}M^{2+}_{x+y}\square_{1-y/3})^{VI}(Si_{3+x}Al_{1-x})^{IV}O_{10}(OH)_2$. As will be shown later, high values of y are observed in low-pressure white micas; therefore, this study deals with the extent of muscovite solid solutions in the system K_2O-$M^{2+}O$-Al_2O_3-SiO_2-H_2O, considering both substitutions (1) and (2), under 2 kbar P_{H_2O}, as a function of temperature between 300 and 700 °C. Two series of experiments were performed, one with M^{2+} = Mg^{2+} and one with M^{2+} = Fe^{2+}. In addition, fluorine was added to the system for some runs. Several other important substitutions are possible in muscovites, especially those involving Fe^{3+}, Ti^{4+}, and interlayer cations; they are not considered here.

Experimental method

The extent of the solid solution domain stable at each temperature has been determined experimentally by using classical methods of hydrothermal synthesis. The starting products were gels of appropriate composition, i.e. having variable values of x and y, prepared according to the method described by Hamilton and Henderson (1968). 100 mg of each gel were introduced into a gold tube together with 15 microlitres of distilled water, before arc welding. The use of cold-seal pressure vessels permitted the simultaneous control of temperature and pressure. The temperature was measured with a thermocouple located inside the wall of the pressure vessel; the accuracy of measurement is estimated to be ±5 °C. The pressure was measured with a Bourdon-type manometer, with an estimated accuracy of ±50 bars. The minimum run duration was chosen as a function of temperature: 8 days above 600 °C, 12 days at 600 °C, 3 weeks at 500 °C, 1 month at 400 °C, and 3 months at 300 °C. Previous work on similar systems (Robert, 1976, 1981) has shown that these durations are satisfactory to obtain reproducible equilibria. For the synthesis of micas in a fluorine-bearing system, KF was added to a starting gel depleted in potassium so as to preserve the bulk potassium stoichiometry of the starting product.

In the iron-bearing system, the starting product was a mixture of two gels, one containing iron as Fe^0 and the other containing iron as Fe^{3+}; the right starting proportion used was $Fe^{3+}/Fe^0 = 3/2$; this technique leads to the rapid attainment of a reproducible equilibrium in which ferrous iron is widely prevalent (Julliot *et al.*, 1985). In addition, the system may be considered to be roughly buffered by the couple Ni-NiO, set by the alloy constituting the pressure-vessel.

After the experiments the products were identified and characterized under the polarizing microscope, by scanning electron microscopy and by X-ray diffraction. The cell dimensions of micas are of interest, and specially the cell parameter $b = 6 \cdot d_{060}$, classically used to characterize micas. The lattice spacing $d_{060,33\bar{1}}$ (given as d_{600} in the tables) was systematically measured, with pure silicon added as an internal standard, the radiations used being Cu-$K\alpha$ (λ = 1.5418 Å) for magnesian micas and Co-$K\alpha$ (λ = 1.7902 Å) for ferrous micas. The micas obtained as a single phase have also been studied by infra-red spectrometry; the results of this study will be given in a forthcoming paper.

The results are represented (fig. 1) in a triangle M^{2+}-Al-Si (atomic proportions; Al = $Al^{IV} + Al^{VI}$. This triangle is a section nearly parallel to the base M^{2+}-Al-Si of a K-M^{2+}-Al-Si tetrahedron representing the experimental system. All the micas

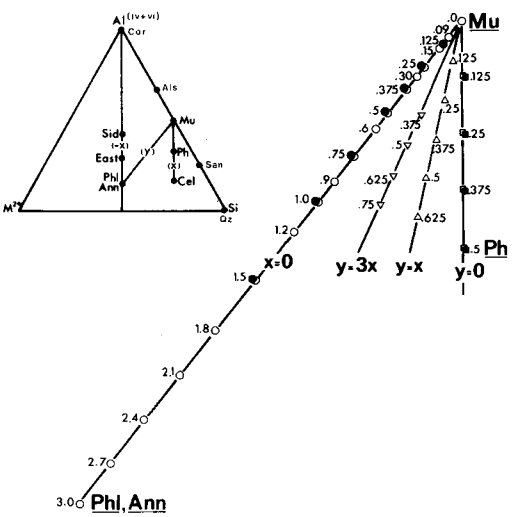

FIG. 1. Positions of mica end members, principal joins and starting experimental compositions in the diagram M^{2+}-Al-Si (atomic proportions). (o) magnesian compositions; (●) ferrous compositions. The sum $x + y = M^{2+}$ is indicated close to the experimental points. Mu = muscovite end member, Ph = phengite, Cel = celadonite end member, Phl,Ann = phlogopite and annite end members, East = eastonite, Sid = siderophyllite, Cor = corundum, Als = aluminosilicate, San = sanidine, Qz = quartz.

studied here belong to this plane, since all of them contain one K atom per formula unit. In this plane three joins are important: the join muscovite–celadonite (x), i.e. the phengitic series—on this join, the micas are purely dioctahedral; the join phlogopite–eastonite (Robert, 1976, 1981) in the magnesian system or annite–siderophyllite (Rutherford, 1973) in the ferrous system—this join is parallel to the previous one and corresponds to purely trioctahedral micas; and the join muscovite–phlogopite (or annite), (y), along which all the micas are solid solutions between dioctahedral and trioctahedral micas.

All the micas situated between the first two joins are solid solutions between dioctahedral and trioctahedral micas. The micas which belong to the join muscovite–phlogopite (or annite) have a constant composition in their tetrahedral layer: Si_3Al.

Experimental results in the magnesian system

The different starting compositions are given in Tables I–IV in terms of x, y, and F content; the run temperature is also indicated in these tables, together with the nature of the final phase assemblages. In the plane M^{2+}–Al–Si, the compositions

Table I. 600°C, 2 kbar, x + y = Mg

Condensed starting material		Phase assemblage	d_{060} (Å), Mu_{ss}
x = 0			
y = 0	F = 0	Mu	1.4992
y = 0.09	F = 0	Mu_{ss}	n.d.
y = 0.15	F = 0	Mu_{ss}	1.5004
y = 0.30	F = 0	Mu_{ss}	1.5012
y = 0.375	F = 0	Mu_{ss}, Phl_{ss}	1.5020
y = 0.60	F = 0	Mu_{ss}, Phl_{ss}	1.5021
y = 0.90	F = 0	Mu_{ss}, Phl_{ss}	1.5023
y = 0.15	F = 0.10	Mu_{ss}	1.5002
y = 0.30	F = 0.20	Mu_{ss}	1.5006
y = 0.60	F = 0.40	Mu_{ss}, Phl_{ss}	1.5011
y = 0.90	F = 0.60	Mu_{ss}, Phl_{ss}	1.5015
y = 1.20	F = 0.80	Mu_{ss}, Phl_{ss}	1.5016
y = 1.50	F = 1.00	Mu_{ss}, Phl_{ss}	n.d.
y = 1.80	F = 1.20	Mu_{ss}, Phl_{ss}	n.d.
y = 2.10	F = 1.40	Mu_{ss}, Phl_{ss}	n.d.
y = 2.40	F = 1.60	Phl_{ss}	
y = 2.70	F = 1.80	Phl_{ss}	
y = 3.00	F = 2.00	F_2-Phl	
y = 0.25	F = 0.50	Mu_{ss}	1.5001
y = 0.50	F = 1.00	Mu_{ss}, Phl_{ss}	1.5000
y = 0.75	F = 1.10	Mu_{ss}, Phl_{ss}	1.4998
y = 1.00	F = 1.20	Mu_{ss}, Phl_{ss}	1.4999
y = 3x			
y + x = 0.375	F = 0	Mu_{ss}, San, (Phl_{ss}?), (Qz)	1.5018
y + x = 0.50	F = 0	Mu_{ss}, Phl_{ss}, San, (Qz)	1.5022
y = x			
y + x = 0.125	F = 0	Mu_{ss}, (San)	n.d.
y + x = 0.25	F = 0	Mu_{ss}, San, (Qz)	n.d.
y + x = 0.375	F = 0	Mu_{ss}, San, Phl_{ss}, (Qz)	n.d.
y = 0			
x = 0.125	F = 0	Mu_{ss}, San, (Qz)	1.5001
x = 0.25	F = 0	Mu_{ss}, San, (Qz)	1.5012
x = 0.375	F = 0	Mu_{ss}, San, Phl_{ss}, Qz	1.5022
x = 0.50	F = 0	Mu_{ss}, San, Phl_{ss}, Qz	1.5022

Table II. 500°C, 2 kbar, x + y = Mg

Condensed starting material		Phase assemblage	d_{060} (Å), Mu_{ss}
x = 0			
y = 0.30	F = 0	Mu_{ss}	1.5017
y = 0.60	F = 0	Mu_{ss}, Phl_{ss}	1.5031
y = 0.90	F = 0	Mu_{ss}, Phl_{ss}	1.5034

Table III. 400°C, 2 kbar, x + y = Mg

Condensed starting material		Phase assemblage	d_{060} (Å), Mu_{ss}
x = 0			
y = 0.30	F = 0.20	Mu_{ss}	1.5008
y = 0.60	F = 0.40	Mu_{ss}, (Phl_{ss})	1.5032
y = 0.90	F = 0.60	Mu_{ss}, Phl_{ss}	1.5047
y = 1.20	F = 0.80	Mu_{ss}, Phl_{ss}	1.5048
y = 1.80	F = 1.20	Phl_{ss}, Mu_{ss}	n.d.
y = 2.10	F = 1.40	Phl_{ss}	
y = 2.40	F = 1.60	Phl_{ss}	
y = 3x			
y + x = 0.375	F = 0	Mu_{ss}	1.5033
y + x = 0.50	F = 0	Mu_{ss}	1.5045
y + x = 0.625	F = 0	Mu_{ss}, (Phl_{ss})	1.5064
y + x = 0.75	F = 0	Mu_{ss}, Phl_{ss}	1.5065
y + x			
y + x = 0.25	F = 0	Mu_{ss}	1.5023
y + x = 0.375	F = 0	Mu_{ss}	1.5036
y + x = 0.50	F = 0	Mu_{ss}, San, (Phl_{ss} ?), (Qz)	1.5049
y + x = 0.625	F = 0	Mu_{ss}, San, Phl_{ss}, (Qz)	1.5074
y = 0			
x = 0.125	F = 0	Mu_{ss}	n.d.
x = 0.25	F = 0	Mu_{ss}, San, (Qz)	1.5023
x = 0.375	F = 0	Mu_{ss}, San, (Qz)	1.5047
x = 0.50	F = 0	Mu_{ss}, San, Phl_{ss}, (Qz)	1.5063

Table IV. 300°C, 2 kbar, x + y = Mg

Condensed starting material		Phase assemblage	d_{060} (Å), Mu_{ss}
x = 0			
y = 0.30	F = 0	Mu_{ss}	1.5021
y = 0.60	F = 0	Mu_{ss}, (Phl_{ss})	1.5058
y = 0.90	F = 0	Mu_{ss}, Phl_{ss}	1.5081
y = 1.20	F = 0	Mu_{ss}, Phl_{ss}	1.5086
y = 1.50	F = 0	Mu_{ss}, Phl_{ss}	1.5088

Notes on Tables I–VI

Principal compositions used in the determination of the compositional range of muscovite and of its phase relations; measured d_{060} (Å) of muscovite solid solutions.

Muscovite solid solutions are given in terms of x, y (see equations (1) and (2) in the text) and F (fluorine content).

Tables I–IV: y and x represent Mg content
Tables V and VI: y and x represent Fe^{2+} content

y, x and F are atoms per formula unit (a./f.u.) on the basis of 11 oxygen equivalents.

Mu : muscovite end member ; Mu_{ss} : muscovite solid solution ; F_2-Phl : fluor-phlogopite end member ; Phl_{ss} : phlogopite solid solution ; Ann_{ss} : Annite solid solution ; San : Sanidine ; Qz : quartz. Parentheses indicate a very minor phase.

Average Δd value is 0.0003 Å at 600°C and slightly greater at lower temperatures ; n.d. : not determined.

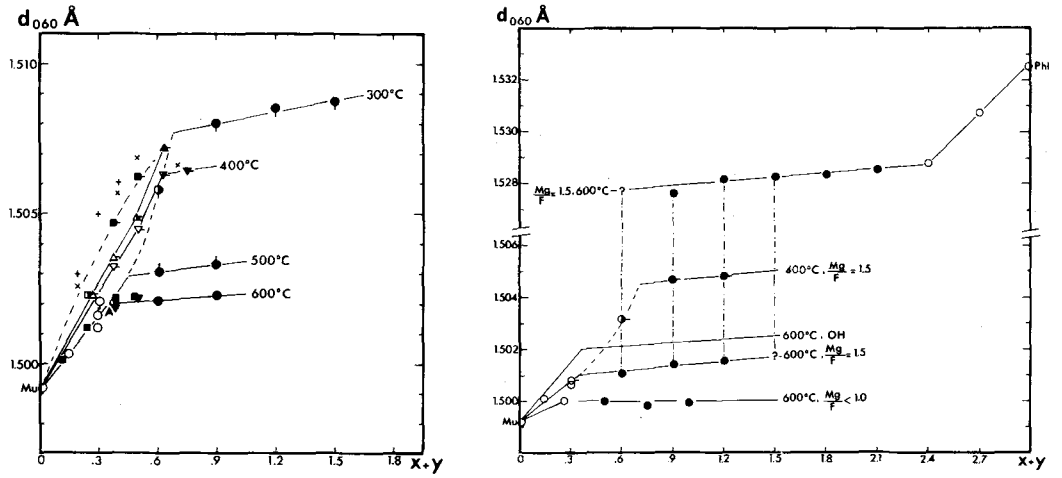

FIGS. 2 and 3. FIG. 2 (*left*). Variation of d_{060} (Å), with $x+y = M^{2+}$ in the OH-bearing muscovite solid solutions, in the magnesian system: (o) $x = 0$; (▽) $y = 3x$; (△) $y = x$; (□) $y = 0$; (o, ▽, △, □) dioctahedral mica only; (●, ▼, ▲, ■) dioctahedral mica plus minor phases; (●, ▼, ▲, ■) polyphase assemblage; (o) 600 °C; (ó) 500 °C; (o-) 400 °C; (o) 300 °C; (+) phengites from Velde (1965); (×) phengites from Massonne (1981). FIG. 3 (*right*). Variations of d_{060} (Å), with $x+y = M^{2+}$ in the (OH,F)-bearing muscovite solid solutions, in the magnesian system. The significance of symbols is the same as in fig. 2. The variation of $d_{060} = f(x+y)$ in the F-free system at 600 °C, 2 kbar, is reproduced (from fig. 2). The variations of $d_{060} = f(x+y)$ in F-bearing phlogopites at 600 °C are also indicated. The tie-lines link the two micas coexisting in the two-phase assemblage.

of the starting products are indicated in fig. 1; the value of $x+y$, i.e. M^{2+}, is given for each point. From fig. 1 it is seen that the experimental points are located on a series of four lines radiating from the muscovite end member. The d_{060} values of the synthetic micas are given in fig. 2 (purely OH micas) and fig. 3 (partial replacement of OH by F), as a function of $x+y$ in the bulk product.

Extent of the solid solution domain of muscovite at 600 °C, 2 kbar. Phase assemblages. In this paper, the terms muscovite and phlogopite (or annite), are used to designate muscovite, phlogopite, annite solid solutions. The text specifies (e.g. muscovite) when end members are concerned. In the OH-bearing system, the solid solution domain of muscovites is very limited at 600 °C. It is restricted to the narrow area defined by points Mu–A–B–E in fig. 4.

Muscovite–phlogopite join. On this join (substitution y), a single dioctahedral mica phase is obtained for $0 \leqslant y \leqslant 0.3$; this phase, whose structural formula for $y = 0.3$ is $K(Al_{1.8}Mg_{0.3}\square_{0.9})(Si_3Al)O_{10}(OH)_2$, is a mixture of the polytypes $1M$ and $2M$. For higher values of y, a trioctahedral mica appears together with the dioctahedral one, and the proportion of trioctahedral mica increases regularly with increasing y, for $0.3 < y \leqslant 2.1$. A minor, unidentified, low refractive index ($n < 1.55$) phase is sometimes present (sanidine?) with the two micas. This phase, which appears at random in runs, is not detectable by X-ray diffraction; it should be noted that it cannot represent more than 1% of the bulk final product when it is present. For $2.4 < y \leqslant 3$, i.e. between point C and the phlogopite end member (fig. 4), a new single phase domain appears, with a trioctahedral mica alone; this agrees with the experimental results of Robert (1976, 1981) on phlogopite solid solutions.

The variation of d_{060} with the composition of muscovites (fig. 2) deserves some comments: d_{060} increases rapidly with the Mg content (i.e. with y), until phlogopite appears (point A, $0.3 < y < 0.375$, fig. 2); for higher values of y, d_{060} still increases with y, but with a much smaller slope. The break at point A (figs. 2 and 4) corresponds to the limit of solid solution of muscovite on the join muscovite–phlogopite. The slight increase of d_{060} with y beyond point A shows that the compositions of muscovite deviate from the join muscovite–phlogopite and can no longer be described by the unique parameter y, but by a combination of x and y. At the same time, d_{060} of the coexisting trioctahedral mica increases in the same proportion. An example of the variation of d_{060} of phlogopite solid solution in the F-bearing system is given in fig. 3. The arrows Mu–A–B and D–C–Phl (fig. 4) show diagrammatically the changes in the compositions of micas obtained from starting gel compositions

ranging from the muscovite to the phlogopite end members. From a starting gel composition having $y = 0.375$, a muscovite with composition close to A coexists with traces of phlogopite with composition close to D; from a starting gel composition having $y = 2.1$, a phlogopite with composition close to C coexists with traces of muscovite with composition close to B (fig. 4).

In the F-bearing system, the extent of solid solution between muscovite and phlogopite (y) is identical to that of the F-free system for the compositions investigated (Table I), whatever the fluorine content. A complete solid solution exists in phlogopite between the hydroxyl and the fluorine end members, but this solid solution is partial in muscovite, with X_F maximum $\simeq 0.3$ at 700 °C, 2 kbar P_{H_2O} (Munoz and Ludington, 1977); for this reason the fluorine content of the starting products have been limited to relatively low values (Table I) for the study of muscovite solid solutions. The studies in the F-bearing systems are based on the hypothesis of an almost complete fixation of fluorine in the solid phase(s); this has been fully verified (Robert, 1981).

The positions of the breaks in the curves $d_{060} = f(M^{2+})$ change very little with F content (fig. 3). It is interesting to note that the progressive replacement of OH by F in micas having a constant cationic composition (i.e. the same y value) results in a decrease of d_{060}, a phenomenon previously noticed in phlogopites (Yoder and Eugster, 1954). This decrease of d_{060} with increasing fluorine content partially balances the increase of d_{060} with increasing Mg, so that, for the high-fluorine micas, the break on the curve is difficult to detect (fig. 3, lower curve).

The muscovite–celadonite join. This join (substitution x) has been investigated in less detail in the present study, because previous studies on phengites by Velde (1965, 1967) are available and we refer to these studies to define the extent of the solid solution on this join; our results are in satisfactory agreement. However, the nature of the phase assemblages obtained deserves attention. According to Velde's work, the most magnesian mica stable at 600 °C, 2 kbar, on the join muscovite–celadonite has the structural formula $K(Al_{1.925}Mg_{0.075}\square)(Si_{3.075}Al_{0.925})O_{10}(OH)_2$; it corresponds to $x = 0.075$ and $y = 0$ in the general formula. The starting compositions having $0.125 \leqslant x \leqslant 0.25$ give the assemblage: muscovite solid solution + sanidine + (quartz).*

This assemblage, in which muscovite is the only mica phase, persists up to $x = 0.375$; for this value of x, traces of phlogopite are detectable. The amount of phlogopite increases regularly with x beyond this value. The existence of a relatively large solid-solution domain between muscovite and phlogopite (y) explains the persistent existence of the assemblage muscovite solid solution + sanidine + (quartz) in the (x) direction. It is noticeable that the appearance of phlogopite in the assemblage occurs for similar values of x (0.375) and y (0.30–0.375); see fig. 4.

A regular increase in d_{060} for muscovites of this polyphase assemblage up to $x = 0.375$ (fig. 2) is noted; above this value no accurate measurement of d_{060} of the mica phase can be obtained because of its overlap with d_{028} of the increasingly abundant sanidine. The following conclusions can be drawn.

Beyond the single-phase domain, the bulk compositions on the join muscovite–celadonite, between E and F (fig. 4) and, more generally, all those belonging to the domain E–F–B, give the assemblage sanidine + (quartz) + a dioctahedral mica solid solution whose composition evolves along the envelope of the solid-solution domain (see the dotted lines, fig. 4).

Beyond point F on the muscovite–celadonite join, and, generally speaking, for all the bulk compositions located inside the triangle C–B–F (fig. 4), a trioctahedral mica solid solution is present.

In the assemblage of four solid phases, 2 micas + feldspar + (quartz), the variance of the system is zero under given T,P conditions, and the composition of each phase is fixed, B for the dioctahedral mica and C for the trioctahedral one.

The solid solution domain at lower temperatures (500, 400, 300 °C). The most complete study of the extent of the solid-solution domain of muscovite was obtained at 400 °C (Table II); at 500 and 300 °C it has been limited to a study of the muscovite–phlogopite join (Tables III and IV). The variation of d_{060} is again shown in fig. 2 (F-free micas) and fig. 3 (F-bearing micas).

The decrease of temperature produces a significant increase in the extent of the solid-solution domain, but the nature of the phase assemblages remains unchanged. Fig. 5 gives details of result obtained at 400 °C, 2 kbar P_{H_2O}. All results, from 300 to 650 °C are shown in fig. 7.

Considering fig. 5, fig. 2 and the series of compositions having $y = 3x$, traces of phlogopite solid solution were detected in the run product for $x + y$

* Quartz has been occasionally detected in the phase assemblages (as indicated by Velde, 1965) in the run products obtained from a starting ratio water/dry gel = 15 wt. %. Some runs were done with the higher starting ratio water/gel = 50 %, and quartz was invariably present in the final products. Therefore it is possible to consider that a part of the minor quartz observed here is a possible quench phase whose amount depends on the solubility of silica in water under the T,P conditions.

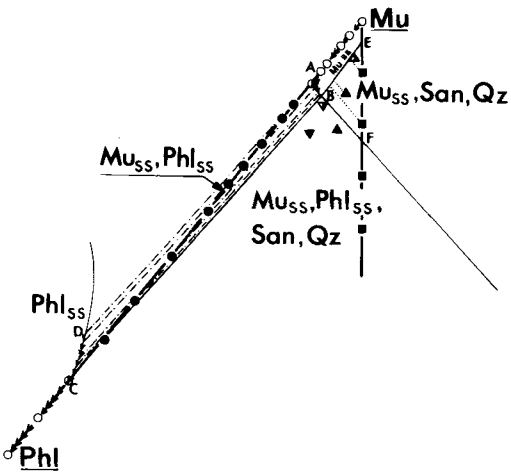

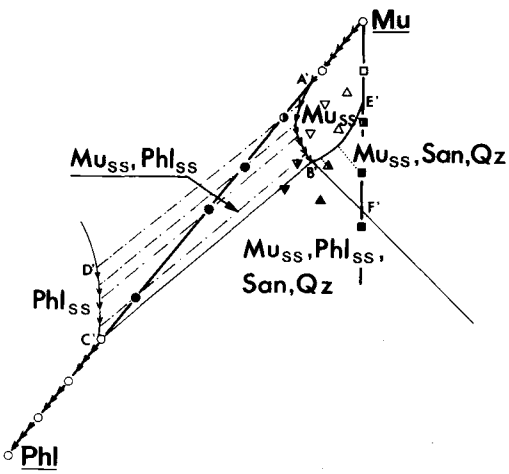

FIGS. 4 and 5. FIG. 4 (*left*). Extent of the muscovite solid-solution field in the magnesian system at 600 °C, 2 kbar, and phase assemblages. FIG. 5 (*right*). Extent of the muscovite solid-solution field in the magnesian system at 400 °C, 2 kbar, and phase assemblages. Same symbols as figs. 2 and 3.

(i.e. Mg) = 0.625, and the amount of trioctahedral mica increased for $x+y = 0.75$. The value $x+y = 0.625$ is also approximately that for which d_{060} stops increasing when a polyphase assemblage appears (two-phase assemblage $Mu_{ss} + Phl_{ss}$, in the present case). This is due to the fact that the line $y = 3x$ passes very close to the extremity (point B', fig. 5) of the solid-solution domain stable at 400 °C, which is not true for the other studied series: $y = 0$, x variable (muscovite-celadonite join); $y = x$; and $x = 0$, y variable (muscovite-phlogopite join).

At 400 °C, after the appearance of a polyphase assemblage, d_{060} of the dioctahedral mica increases, rapidly at first and then with a lower slope (fig. 2) beyond the break on the curve $d_{060} = f(x+y)$. At 400 °C, as at 600 °C, the composition of the dioctahedral mica solid solution, in the polyphase assemblage, evolves along the envelope of the solid-solution domain from A' to B' for the bulk compositions located on the join muscovite-phlogopite ($x = 0$), and from E' to B' for those having $y = 0$ (muscovite-celadonite join) and $y = x$. The same behaviour is observed for the compositions on the muscovite-phlogopite join at 500 and 300 °C (fig. 2).

Data on phengites of lower and/or higher water pressure origin, from Velde (1965) and Massonne (1981) are plotted in fig. 2. A steeper slope of the line $d_{060} = f(x+y)$ along the join muscovite-celadonite, than along the join muscovite-phlogopite, is observed. Intermediate compositions, $y = x$ and $y = 3x$, show an intermediate behaviour. This was previously observed in synthetic phlogopites (Robert, 1973); for the same Mg content, the vacancy-rich phlogopites, i.e. solid solution phlogopite-muscovite, have a cell parameter b significantly greater than those with no vacant trioctahedral site, i.e. solid solution phlogopite-eastonite. This behaviour is closely related to the size of the vacant octahedral sites (1 Å between the centre of the vacant $M(1)$ site and the surrounding oxygens in muscovite) which are significantly larger than the ionic radii of octahedrally coordinated cations; 0.72 Å for Mg^{2+} and 0.53 Å for Al^{3+} (Shannon and Prewitt, 1969, 1970).

Experimental data for $T > 600$ °C, at 2 kbar P_{H_2O}. At these higher temperatures, the aim of the experiments was to determine the stability of dioctahedral mica solid solutions on the muscovite-phlogopite join, compared with the stability of the muscovite end member.

The muscovite end member decomposes into the assemblage sanidine + corundum + vapour, between 650 and 675 °C, at 2 kbar P_{H_2O}. This temperature range is similar to that established by Chatterjee and Johannes (1974) for the same reaction (640-660 °C) under the same water pressure.

The upper stability limits of the compositions $K(Al_{1.9}Mg_{0.15}\square_{0.95})(Si_3Al)O_{10}(OH)_2$ and $K(Al_{1.9}Mg_{0.15}\square_{0.95})(Si_3Al)O_{10}((OH)_{1.9}F_{0.1})$, i.e. $x = 0$ and $y = 0.15$, are in the same temperature range. The composition $K(Al_{1.915}Mg_{0.125}\square_{0.96})(Si_3Al)O_{10}((OH)_{1.75}F_{0.25})$, i.e. $x = 0$; $y = 0.125$; $X_F = 0.125$, is still stable at 700 °C (present work), as also was the F-bearing ($X_F \simeq 0.3$) muscovite end member (Munoz and Ludington, 1977). Apparently,

no magnesian composition belonging to the muscovite-phlogopite join is stable at higher temperature than the muscovite end member itself, but the presence of fluorine in the system stabilizes muscovite solid solutions at higher temperatures. F-bearing muscovites with $x = 0$ and $0 \leqslant y \leqslant 0.125$ are still stable at 700 °C.

Experimental results in the ferrous system

The solid solutions of muscovite in the ferrous system have been studied in less detail than in the magnesian equivalent, being confined to compositions on the joins muscovite–annite ($x = 0$; y variable) and muscovite–celadonite (x variable; $y = 0$) in the purely hydrous and in the F-bearing systems, at 600 °C and 400 °C, at 2 kbar P_{H_2O} (Tables V and VI). The compositions investigated are plotted in fig. 6, together with the observed solid-solution domains; the short-dashed lines indicate extrapolations. Owing to the unavoidable presence of minor Fe^{3+}, the experimental results are less accurate in the ferrous system and traces of accessory phases frequently appear, even in the stable composition domain of the dioctahedral mica solid solution. These phases, among which only sanidine could be identified, never represent more than about 1–2 % of the final product. On the other hand, the observation of run products under the polarizing microscope is made easier, particularly on the join muscovite–annite, because of the bronze-green colour of annite solid solutions.

The geometry of the solid-solution domains and the nature of the phase assemblages in the ferrous system are qualitatively identical to those of the magnesian one, but the extent of the solid-solution domain of muscovite is much more restricted in the ferrous system, at the same temperatures.

In the F-free system, on the join muscovite–annite, traces of trioctahedral mica are detected for $y = 0.25$ at 600 °C and for $y = 0.375$ at 400 °C. The behaviour of d_{060} with increasing y is similar to that observed in the magnesian system: a break on the curve $d_{060} = f(y)$ occurs at 600 °C but no visible break occurs up to $y = 0.5$ at 400 °C. For higher values of y, in run products prepared at 400 °C, the weak intensity of the peak and its interference with d_{061} and $d_{33\bar{2}}$ of the associated trioctahedral mica prevents any accurate measurement of d_{060} of the dioctahedral mica.

The dioctahedral mica solid solution deviates from the join muscovite–annite at point A (fig. 6) and follows the line A–B, similar to point A and line

Table V. 600°C, 2 kbar, x + y = Fe^{2+}

Condensed starting material		Phase assemblage	d_{060} (Å), Mu_{ss}
x = 0			
y = 0.125	F = 0	Mu_{ss}	1.5001
y = 0.25	F = 0	Mu_{ss}, (Ann_{ss})	1.5009
y = 0.375	F = 0	Mu_{ss}, Ann_{ss}	1.5011
y = 0.50	F = 0	Mu_{ss}, Ann_{ss}	1.5013
y = 0.75	F = 0	Mu_{ss}, Ann_{ss}	1.5018
y = 1.00	F = 0	Mu_{ss}, Ann_{ss}	n.d.
y = 1.50	F = 0	Ann_{ss}, (San)	
y = 0.125	F = 0.25	Mu_{ss}	1.5002
y = 0.25	F = 0.50	Mu_{ss}, (Ann_{ss})	1.5016
y = 0.375	F = 0.75	Mu_{ss}, Ann_{ss}	1.5016
y = 0.50	F = 1.00	Mu_{ss}, Ann_{ss}	1.5034
y = 0.75	F = 1.00	Mu_{ss}, Ann_{ss}	n.d.
y = 1.00	F = 1.00	Mu_{ss}, Ann_{ss}	n.d.
y = 1.50	F = 1.00	Ann_{ss}, (San ?)	
y = 0			
x = 0.125	F = 0	Mu_{ss}, San, (Qz)	n.d.

Table VI. 400°C, 2 kbar, x + y = Fe^{2+}

Condensed starting material		Phase assemblage	d_{060} (Å), Mu_{ss}
x = 0			
y = 0.25	F = 0	Mu_{ss}	1.5009
y = 0.375	F = 0	Mu_{ss}, (Ann_{ss})	1.5024
y = 0.50	F = 0	Mu_{ss}, Ann_{ss}	1.5039
y = 0.75	F = 0	Mu_{ss}, Ann_{ss}	n.d.
y = 1.00	F = 0	Mu_{ss}, Ann_{ss}	n.d.
y = 1.50	F = 0	Ann_{ss}	
y = 0			
x = 0.125	F = 0	Mu_{ss}, (San)	n.d.
x = 0.25	F = 0	Mu_{ss}, San, (Qz)	n.d.
x = 0.375	F = 0	Mu_{ss}, San, (Qz)	n.d.
x = 0.50	F = 0	Mu_{ss}, San, Ann_{ss}, (Qz)	n.d.

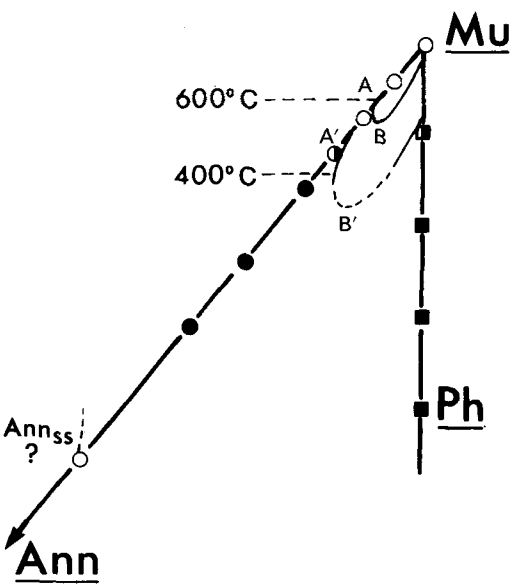

FIG. 6. Extent of the muscovite solid-solution field in the ferrous system at 400 and 600 °C. The dotted line indicates an extrapolation. Symbols are for 400 °C, as in fig. 5.

A–B of the magnesian system at 600 °C (fig. 4). Points A′ and B′ in fig. 6 correspond to points A′ and B′ in fig. 5 (400 °C). On the join muscovite–celadonite, there is practically no solid solution at 600 °C, 2 kbar, as shown earlier by Velde (1965). At 400 °C, there is some solid solution, up to x slightly less than to 0.125 (Table V). The presence of fluorine in the system ($0.5 \leqslant Fe/F \leqslant 1.5$, atomic ratio) does not significantly change the results on the join muscovite–annite (Table V).

The upper stability limit of a mica whose structural formula is $K(Al_{1.915}Fe^{2+}_{0.125}\square_{0.96})(Si_3Al)O_{10}(OH)_2$ ($x = 0$; $y = 0.125$; $X_F = 0$) is in the range 650–675 °C, but a mica having the same cationic composition and $(OH)_{1.75}F_{0.25}$ ($X_F = 0.125$) is stable up to 700 °C, like its magnesian equivalent.

Summary of experimental results. Similarities between dioctahedral and trioctahedral micas solid solutions

Fig. 7 shows the extent of the solid-solution domains of dioctahedral micas, stable from 300 to 650 °C, in the system K_2O–MgO–Al_2O_3–SiO_2–H_2O–(HF) at 2 kbar P_{H_2O} and, for comparison, the solid-solution domain of trioctahedral micas in the same system, from 600 to 1000 °C, at 1 kbar P_{H_2O} (Robert, 1981).

One notes the significant and asymmetrical reduction of the extents of the solid-solution domains with increasing temperature, for both dioctahedral and trioctahedral micas. For both families, the most stable composition at high temperature is that of the pure end member, muscovite in the dioctahedral family and phlogopite in the trioctahedral one. These facts are discussed in terms of crystal-chemical considerations in Robert (1981).

The behaviour of the two families is thus qualitatively identical: with increasing temperature, under a constant water pressure, the most stable compositions are those lying along the join muscovite–biotite. For micas on this join, the composition of the tetrahedral layer in Si_3Al, which corresponds to regular (isometric) tetrahedra and to the most stable structures in the system studied, for crystal-chemical reasons (Robert, 1981).

The behaviour of ferrous dioctahedral micas is qualitatively identical to that of magnesian dioctahedral micas with increasing temperature (compare fig. 7 with fig. 6). However, the extent of the solid-solution domain is much more reduced in the ferrous system; roughly, the extent of the stable domain at 400 °C in the ferrous system corresponds to the stable domain at 550 °C in the magnesian one. Fluorine does not change the extent of the solid-solution domain but raises the upper stability limit by about 50 °C.

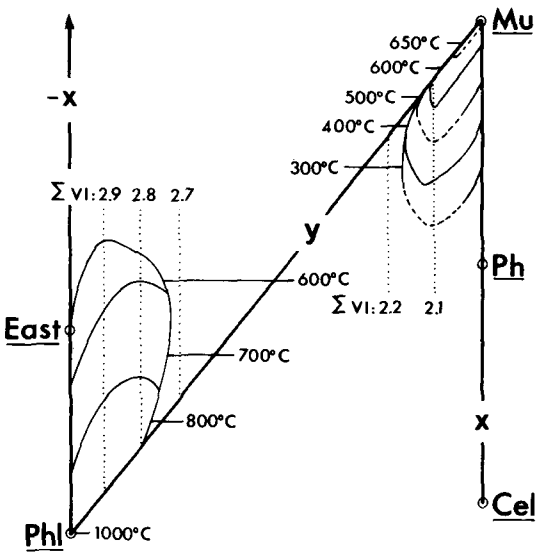

FIG. 7. Summary of experimental results on dioctahedral micas in the magnesian system (this work) and data on phlogopite solid solutions from Robert (1981). The dashed lines indicate extrapolations.

Application to natural Li-free white micas

This comparison focuses only on high-temperature, low-pressure (< 5 kbar) muscovites, typically primary granitic muscovites, and on low-temperature (< 500 °C), low-pressure ones, typically white micas from hydrothermally altered granitic rocks. Both types can be considered as having crystallized in T,P environments closer to our experimental conditions than most micas of metamorphic origin. In the white micas from metamorphic rocks, the phengitic substitution (x) is prevalent in most cases, $x \geqslant y$ (Massonne, 1981), for the fixation of divalent cations.

Muscovites from the two-mica granites. The compositions of a set* of Li-free (or Li-poor, < 300 ppm) primary† and some secondary muscovites from the leucogranitic massif of Goulles (French Massif Central) have been selected for this comparison and plotted in a diagram M^{2+}–Al–Si (fig. 8*a*). Most natural muscovites have very com-

* A hundred analyses of muscovites from Goulles massif (French Massif Central), microprobe and wet chemical analysis on separated micas, are available from the authors on request.

† See Miller *et al.* (1981), Monier *et al.* (1984), and Speer (1984) for discussion on primary, magmatic, and secondary, postmagmatic, muscovites.

plex compositions and do not lie in the plane M^{2+}–Al–Si, due to additional substitutions involving Fe^{2+}, Ti^{4+}, and $\square^{XII}$ (interlayer vacancy). The substitutions can be written $Al \rightleftharpoons Fe^{3+}$ (3), $2Al^{VI} \rightleftharpoons Ti^{VI},(M^{2+})^{VI}$ (4), Monier and Robert (1985) and $K^{XII},Al^{IV} \rightleftharpoons \square^{XII},Si^{IV}$ (5), Monier (1985). In the calculation these three substitutions have been corrected for before plotting, in order to give prominence to the two substitutions, x and y, of interest in the present work. The extents of substitutional mechanisms (4) and (5) can be deduced from the microprobe analysis. The substitutional mechanism (3) involves Fe^{3+}; FeO–Fe_2O_3 determinations have been performed by classical wet analysis on some separated primary muscovites. Their Fe^{3+} content is rather constant and close to 0.05 atoms per formula unit (per 11 oxygens); this constancy allows reasonable estimation of the Fe^{2+}/Fe^{3+} ratio from microprobe analysis.

The range of compositions of these primary muscovites is very restricted (fig. 8*a*, *b*) and lies along the muscovite–biotite join ($x \simeq 0$), close to the muscovite end member ($y \leqslant 0.15$).

Except for the plagioclase, the mineralogical composition of two-mica granites is comparable with the two micas + sanidine + quartz experimental assemblage. In such an assemblage, the composition of the muscovite solid solution is fixed for given T and P in this simplified experimental model system: points B, fig. 4, and B′, fig. 5. According to Velde (1965, 1967) the effect of pressure in the range 2–5 kbar on the extent of the solid-solution domain of muscovite above 600 °C is minor. Therefore, our experimental results obtained at 2 kbar P_{H_2O} can be used to estimate the temperature of crystallization of primary granitic muscovites; a range of pressure 2–5 kbar is commonly assumed for the crystallization of two-mica granites (Lameyre, 1973; Floc'h, 1979; Anderson and Rowley, 1981; Le Fort, 1981; Miller *et al.*, 1981). From the present experimental work, one can estimate a minimum temperature of 650 °C for the crystallization of these primary muscovites, which is in satisfactory agreement with their magmatic origin.

The presence of octahedrally co-ordinated divalent cations in apparently primary plutonic muscovites was previously considered to be inconsistent with a high-temperature and relatively low-pressure origin (see the discussion by Miller *et al.*, 1981) because the phengitic substitution, which was considered as the only possible mechanism for the fixation of Mg^{2+} and Fe^{2+} in muscovite, is almost non-existent above 650 °C in the pressure range 2–5 kbar (Velde, 1965, 1967). Our experimental results in the (x,y) plane, showing a lack of symmetry of the solid-solution domain at high temperature, provide an explanation of this apparent contradiction.

Low-temperature muscovites. We have plotted in fig. 8*a* the compositions of white micas of various origins, taken from the literature, and considered as

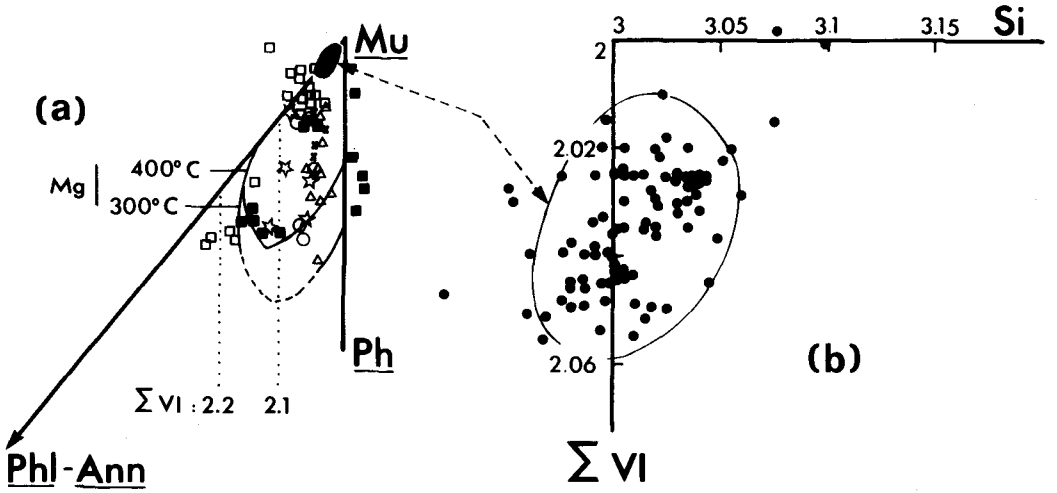

FIG. 8. (*a*) Plot of compositions of various natural muscovites in the diagram M^{2+}–Al–Si: (●) primary (magmatic) granitic muscovites; (×) muscovites from hypothermal veins (Neiva, 1982); (○) muscovites from quartz-carbonate veins in an altered granite (Burnol *et al.*, 1980); (*) muscovites from altered zones associated with porphyry copper deposits from Peru (Le Bel, 1979*a*, *b*); (△) ditto, from British Columbia, Canada (Johan and Le Bel, 1980); (□) muscovites from hydrothermally altered granites from French Armorican Massif (Meunier and Velde, 1982); (■) ditto, from French Massif Central (Dudoignon and Meunier, 1984). (*b*) Compositions of primary (magmatic) granitic muscovites from fig. 8*a* replotted as Si versus ΣVI (octahedral occupancy); see text.

being of low-temperature ($\leqslant 400\,^{\circ}C$) occurrence. All these muscovites are associated with a quartz-feldspar assemblage, with or without biotite, which make them close to the experimental systems of this work. But, for these late muscovites, the nature of the paragenetic equilibria is poorly known, which limits the possibilities of accurate geothermometry from their composition.

In these low-temperature micas, the amount of interlayer H_3O^+ can be important but is generally unknown; in order to avoid too tentative corrections, we only considered those muscovites having $(K + Na) \geqslant 0.9$ atoms per formula unit. Moreover, for most of these micas, the Fe^{2+}/Fe^{3+} ratio is not known; iron is considered to be divalent, but, if some Fe^{3+} is present, the substitution y, i.e. the trioctahedral component in the muscovite solid solution, is overestimated. Therefore, in a general way, the positions of these compositions in the diagram M^{2+}–Al–Si are less precise than those of plutonic muscovites considered previously.

Most of the compositions lie inside the domain of solid solution stable at 300 °C, in the experimental magnesian system. Both substitutions x and y are important and required to describe the compositions. The substitution y can be as high as 0.6 (muscovite from a hydrothermally altered granite studied by Meunier and Velde, 1982), which corresponds to 2.2 octahedral cations per formula unit. To interpret this high octahedral occupancy, these authors suggested the possible presence of traces of inframicroscopic biotite, but, our experimental data allow an alternative explanation in terms of pure white micas with high octahedral occupancy, typical of low-temperature muscovite solid solutions.

Acknowledgements. The authors are indebted to B. Velde for helpful suggestions about low-temperature muscovites. One of us (G.M.) thanks the Commissariat à l'Energie Atomique (C.E.A.-D.A.M.N.) for financial support.

REFERENCES

Anderson, J. L., and Rowley, M. C. (1981) *Can. Mineral.* **19,** 83–101.

Burnol, L., Le Bel, L., and Lougnon, J. (1980) *Chronique de la Recherche Minière*, Ed. B.R.G.M., France, no. 455, 36–59.

Chatterjee, N. D., and Johannes, W. (1974) *Contrib. Mineral. Petrol.* **48,** 89–114.

Crowley, M. S., and Roy, R. (1964) *Am. Mineral.* **49,** 348–63.

Dudoignon, P., and Meunier, A. (1984) Colloquium '*Géologie profonde de la France*', Doc. B.R.G.M. no. 81-8, Ed. B.R.G.M., France, 87–107.

Floc'h, J. P. (1979) *Bull. B.R.G.M.*, France, Section 1, no. 2, 89–107.

Green, T. H. (1981) *Contrib. Mineral. Petrol.* **78,** 452–8.

Hamilton, D. L., and Henderson, C. M. B. (1968) *Mineral. Mag.* **36,** 832–8.

Johan, Z., and Le Bel, L. (1980) *Minéralisations liées aux granitoïdes*, 26e C.G.I., Paris, 95–119.

Julliot, J.-Y., Volfinger, M., and Robert, J.-L. (1986) Submitted to *Tschermaks Mineral. Petr. Mitt.*

Lameyre, J. (1973) *Bull. Soc. Géol. France*, **7,** XV, 3–4, 288–95.

Le Bel, L. (1979*a*) Thèse d'Etat, Univ. Lausanne, Switzerland, 160 pp.

——(1979*b*) *Bull. Minéral.* **102,** 35–41.

Le Fort, P. (1981) *J. Geophys. Res.* **86,** B 11, 10545–68.

Massonne, H. J. (1981) Thesis, Bochum, F.R.G., 211 pp.

Meunier, A., and Velde, B. (1962) *Clay Minerals*, **17,** 285–99.

Miller, C. F., Stoddard, E. F., Bradfish, L. J., and Dollase, W. A. (1981) *Can. Mineral.* **19,** 25–34.

Monier, G. (1985) Thèse d'Etat, Univ. Orléans, France, 299 pp.

——and Robert, J.-L. (1985) *Neues Jahrb. Mineral. Abh.* **152,** 147–61.

——Mergoil-Daniel, J., and Labernardiere, H. (1984) *Bull. Minéral.* **107,** 55–68.

Munoz, J. L., and Ludington, S. D. (1977) *Am. Mineral.* **62,** 304–8.

Neiva, A. M. R. (1982) *Metallization Associated with Acid Magmatism* (A. M. Evans, ed.). Wiley, New York, 243–59.

Robert, J.-L. (1973) Thèse 3e cycle, Univ. Paris Sud, France, 73 pp.

——(1976) *Chem. Geol.* **17,** 195–212.

——(1981) Thèse d'Etat, Univ. Paris XI, France, 206 pp.

Rutherford, M. J. (1973) *J. Petrol.* **14,** 159–80.

Shannon, R. P., and Prewitt, C. T. (1969) *Acta Crystallogr.* B **25,** 925–46.

——————(1970) Ibid. B **26,** 1046–8.

Speer, J. A. (1984) Reviews in Mineralogy M.S.A. Micas. Bailey Ed., **13,** 299–356.

Velde, B. (1965) *Am. J. Sci.* **263,** 886–913.

——(1967) *Contrib. Mineral. Petrol.* **14,** 250–8.

——(1980) *Am. Mineral.* **65,** 1277–82.

Yoder, H. S., and Eugster, H. P. (1954) *Geochim. Cosmochim. Acta*, **6,** 157–85.

[*Manuscript received 2 April 1985; revised 28 October 1985*]